MULTIPLE-ARRAY DETECTION, ASSOCIATION AND LOCATION OF INFRASOUND AND SEISMO-ACOUSTIC EVENTS – UTILIZATION OF GROUND-TRUTH INFORMATION

Stephen J. Arrowsmith[1], Il-Young Che[2], Christopher T. Hayward[3], Junghyun Park[3], and Brian W. Stump[3]

Los Alamos National Laboratory[1], Korea Institute of Geoscience and Mineral Resources[2]
and Southern Methodist University[3]

Sponsored by the Air Force Research Laboratory and the National Nuclear Security Administration

Award Nos. DE-AC52-06NA25396[1] and FA8718-08-C-008[2,3]
Proposal No. BAA08-65

ABSTRACT

This work is intended to provide automated methodology for processing seismic and infrasound data from seismo-acoustic arrays and to apply the methodology to regional networks for validation with ground truth information. As reported last year, the project has developed automated techniques for detecting, associating and locating infrasound signals. Work reported this year focuses on refinement of both the detection and location component of the program. Ground truth information developed on the Korean Peninsula is further used to refine the methodology.

New location developments are underway. We are incorporating an infrasonic grid-search location method into a Bayesian framework that provides conditional probabilities on the location given the observed data (inter-array time delays and backazimuths) and a prior distribution. The prior provides ancillary information on the event location, which can be as simple as empirical bounds on backazimuth deviations and group velocities. However, we are investigating extending this simple approach through the use of a 3D ray-tracing algorithm to impose more specific constraints based on available atmospheric specifications.

Finally a set of ground truth seismo-acoustic events have been developed for the Korean Peninsula and include a large number of events from a limestone quarry in the Republic of Korea. In-mine seismic and acoustic observations provide the basis of the detailed ground truth. These events occur daily with multiple events on active days and span nearly two years, providing the basis of assessing spatial and temporal variations in propagation path, including variations in backazimuth as well as phase and group velocity. The reported analyses of these data provide empirical bounding constraints for the location algorithm that is under development.

OBJECTIVES

There are two primary objectives to our effort on the second year of this contract. Each objective builds on the automatic algorithms for detection, association, and location of infrasound events developed in the first year of this project.

- **Development of an infrasound location algorithm with a firm statistical basis**. This objective is a natural extension to the bounding-constraint algorithm developed in Year 1. We formulate a scheme for calculating likelihood values at each node in the grid search method based on the agreement between observed and predicted values for backazimuth and arrival time. This scheme provides the opportunity to compute robust confidence bounds on infrasound locations.
- **Preliminary analysis of infrasound propagation effects using ground-truth data from Korea.** The groundt ruth dataset being acquired for this project provides an opportunity to test and validate new automated algorithms. We report on the preliminary analysis of this dataset, highlighting the effect of seasonal variations in atmospheric winds on travel-times in the Korean peninsula. Propagation path variations such as those documented in this study can be incorporated into the location algorithm.

RESEARCH ACCOMPLISHED

Infrasound Location Algorithm

We are currently extending the grid-search based infrasound location methodology of Arrowsmith et al. (2008a), discussed in last years proceedings (Arrowsmith et al., 2008b), by incorporating it into a Bayesian framework. This development enables us to compute non-ellipsoidal confidence bounds on the event location using two constraints: arrival times $\mathbf{t} = [t_1,...,t_n]$ and backazimuths $\theta = [\theta_1,...,\theta_n]$.

Bayes' theorem is given by:

$$P(t_0,x_0,y_0,v|\mathbf{t},\theta) = \frac{P(\mathbf{t},\theta|t_0,x_0,y_0,v)}{P(\mathbf{t},\theta)} P(t_0,x_0,y_0,v). \quad (1)$$

First, we formulate the value of the *likelihood function*, $P(\mathbf{t},\theta|t_0,x_0,y_0,v)$ at each point in our parameter space. We define our likelihood function as:

$$P(\mathbf{t},\theta|t_0,x_0,y_0,v) = \prod_i \Theta(\mathbf{t},\theta|t_0,x_0,y_0,v) \prod_i \Phi(\mathbf{t},\theta|t_0,x_0,y_0,v) \quad (2)$$

where

$$\Theta_i(t,\theta|t_0,x_0,y_0,v) = \frac{1}{\sqrt{2\pi(\sigma_\theta^2+\sigma_\kappa^2)}} \exp\left[-\frac{1}{2}\left(\frac{\gamma_i^2}{\sigma_\theta^2+\sigma_\kappa^2}\right)\right] \quad (3)$$

and

$$\Phi_i(t,\theta|t_0,x_0,y_0,v) = \frac{1}{\sqrt{2\pi(\sigma_\phi^2)}} \exp\left[-\frac{1}{2}\left(\frac{\varepsilon_i}{\sigma_\phi}\right)^2\right] \quad (4)$$

are the individual likelihoods for the i^{th} array, based on backazimuth and arrival time constraints respectively .The residual terms, γ_i and ε_i, are given by:

$$\gamma_i = \theta_i - \arctan\left(\frac{y_i - y_0}{x_i - x_0}\right) \quad (5)$$

and

$$\varepsilon_i = t_i - \left(t_0 + \frac{\sqrt{(x_i - x_0)^2 + (y_i - y_0)^2}}{v} \right) \quad (6)$$

where the i^{th} array is located at (x_i, y_i), (x_0, y_0, t_0) represents a point and time in our parameter space, and v represents the group velocity that is assumed to be constant at all arrays in the likelihood term.

The uncertainties in backazimuth, σ_θ and σ_κ, represent the standard deviation in the measurement error (a function of array geometry and F-K approach) and the standard deviation in the error produced by the wind respectively. Similarly, the uncertainty in arrival time estimation is denoted by σ_ϕ.

We impose physical constraints on the model parameters in the Bayesian prior term, $P(t_0, x_0, y_0, v)$, as follows:

$$P = \begin{cases} \text{positive constant} & 0.22 \le v \le 0.34 \\ 0 & \text{otherwise} \end{cases}. \quad (7)$$

This constraint assures that the group velocity associated with our solution (x_0, y_0, t_0) lies within the infrasonic range (for direct waves through to thermospheric returns).

The final solution (or posterior), $P(t_0, x_0, y_0, v | \mathbf{t}, \theta)$, is the likelihood of the event location and origin time given our observed data (arrival times and backazimuths). This likelihood is a function that spans some pre-defined geographic region and time window. We apply a grid-search method in order to find the location and origin time associated with the maximum likelihood, with confidence regions defined by the likelihood distribution.

Example

We apply our Infrasonic Bayesian Locator (IBL) to a ground-truth rocket motor explosion recorded at three arrays in Utah (Stump et al., 2007). This event is discussed in Arrowsmith et al. (2008a) and is summarized in Table 1. The known station and event geometry is shown in Figure 1, in addition to the calculated likelihood function Θ – based on backazimuth constraints only – as a function of x and y with t_0 and v fixed at their optimum values. Figure 2 is similar to Figure 1 except that the arrival-time based likelihood function, Φ, is plotted for comparison.

Table 1. Summary of the Utah Test and Training Range explosion ground truth and observations used in this article to illustrate the IBL algorithm.

Ground truth data	**Location**	41.13152°N, 112.89577°W	
	Origin Time	2007/08/27 20:43:12.0	
Observations	**BGU**	Arrival-time	2007/08/27 20:44:27
		Backazimuth	30.96°
	EPU	Arrival-time	2007/08/27 20:45:35
		Backazimuth	237.80°
	NOQ	Arrival-time	2007/08/27 20:47:17
		Backazimuth	304.22°

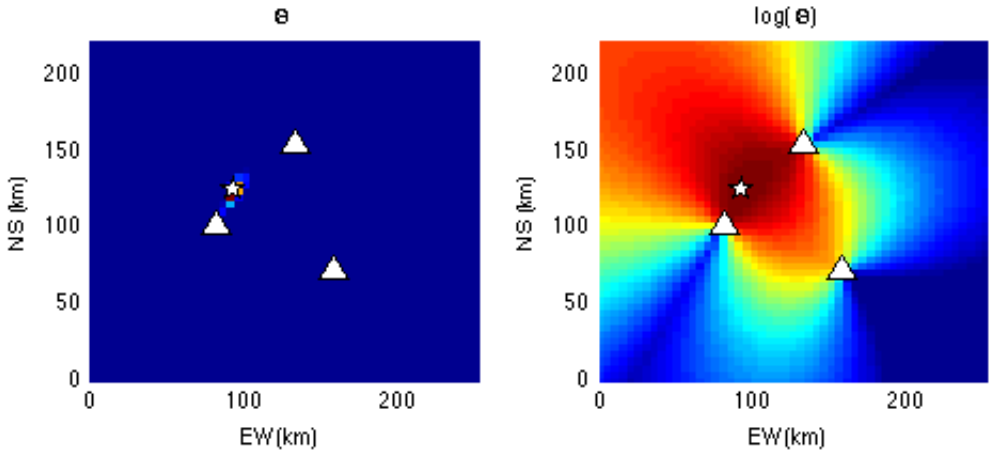

Figure 1. Solutions obtained for the Utah Test and Training Range explosion summarized in Table 1. Left: Plot of the backazimuth function Θ over x and y with t_0 and v fixed at their optimum values. Right: Plot of the natural logarithm of Θ, again with t_0 and v fixed at their optimum values.

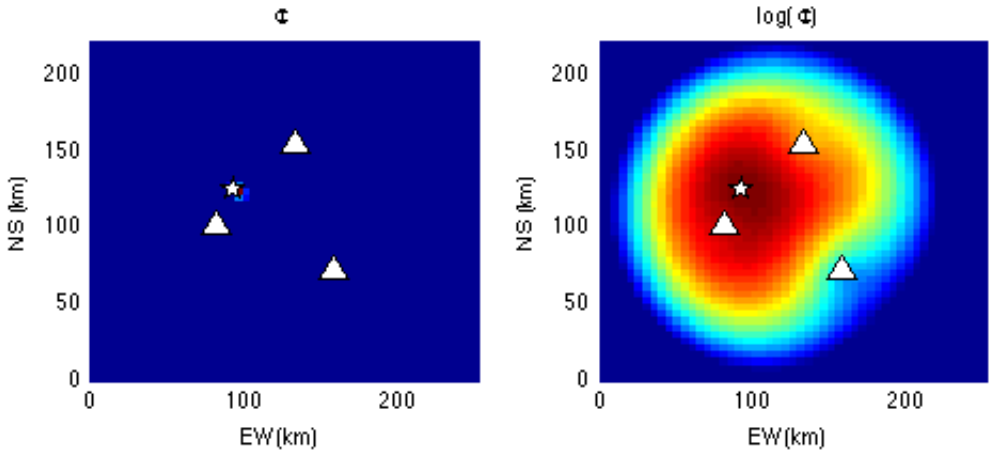

Figure 2. Left: Plot of the arrival time function Φ over x and y with t_0 and v fixed at their correct values. Right: Plot of the natural logarithm of Φ, again with t_0 and v fixed at their optimum values.

The posterior likelihood function (obtained using Bayes' theorem, outlined above) is shown in Figure 3. It is interesting to note that, whereas in Figures 1 and 2 (for backazimuth and travel-time constraints individually) we obtain ellipses, in Figure 3 (once these separate constraints have been effectively combined) we observe a circular region that is better constrained. This result highlights the value of incorporating both backazimuth and arrival time constraints into the solution.

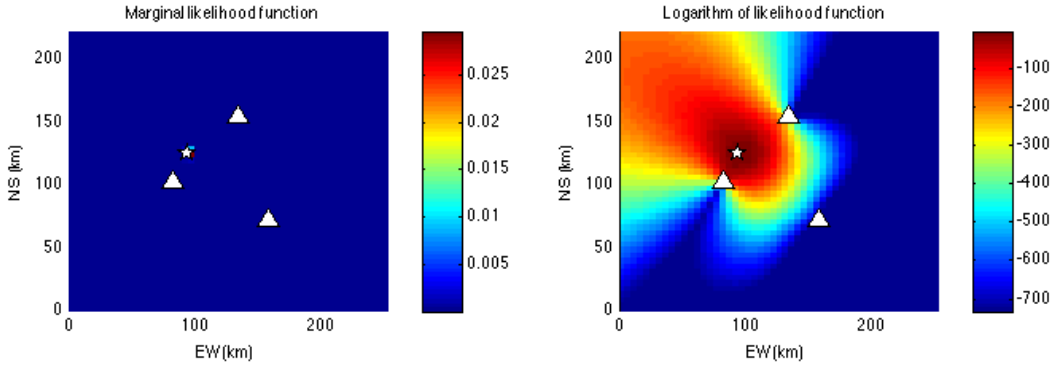

Figure 3. Left: The posterior likelihood function of the variables x_0 and y_0. For this array geometry, the likelihood contours produced by the backazimuths run perpendicular to those produced by the arrival times. The result, seen in this figure, is a well-constrained, circular source region. Right: The natural logarithm of the same posterior likelihood function.

Collection of Long-Term Ground-Truth Events from a Limestone Mine in Korea

Surface blasting activities at industrial mines are good examples of point sources that produce impulsive infrasonic signals. Well-defined blasting information can be utilized to study the characteristics of infrasound propagation in the atmosphere and to verify infrasonic source location methods. In particular, long-term collection of ground-truth events from a mine, conducting daily blasting, provides the basis for assessing spatial and temporal variations of infrasound propagation depending on seasons.

Figure 4(a) shows the locations of several seismic stations (black triangles) and two seismo-acoustic arrays (CHNAR and ULDAR) in South Korea. The inner box illustrates the distribution of seismic events near the east coast of South Korea from 2005 to 2006. The Korea Earthquake Monitoring System (KEMS) reviewed more than 900 events most with seismic magnitudes of less that M_L 2.0. Of these events, those followed by distinct infrasonic signals detected by infrasound arrays were discriminated as surface explosions, not earthquakes, and are marked by yellow circles in the figure. A field survey identified a large open-pit limestone mine (red dot in the figure) in the scattered distribution of these seismic events. This mine blasts several tons of explosives nearly every working day and can be considered as an infrasonic bell since many infrasonic signals from the mine have been recorded at the seismo-acoustic arrays in Korea.

Two temporary seismo-acoustic stations were deployed approximately ~300 m apart from the blasting point during two years starting from April 2007 in order to collect detailed ground-truth information at the mine. Three-component seismometers and acoustic sensors were used to document the sources. The acoustic sensor was connected to a wind-noise reducer. Seismic and acoustic data were digitized at 100 samples per second.

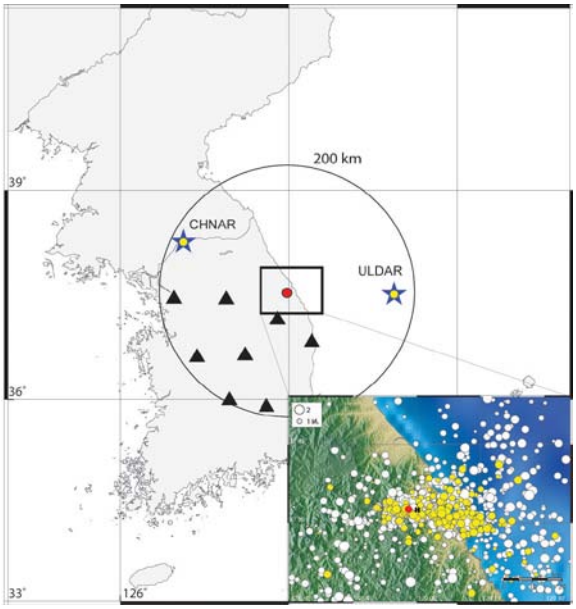

Figure 4. (a) Locations of the mine (red dot), seismic stations (black triangles), and infrasound arrays (CHNAR, ULDAR). Inner box shows distribution of seismic events around the mine in 2005-2006.

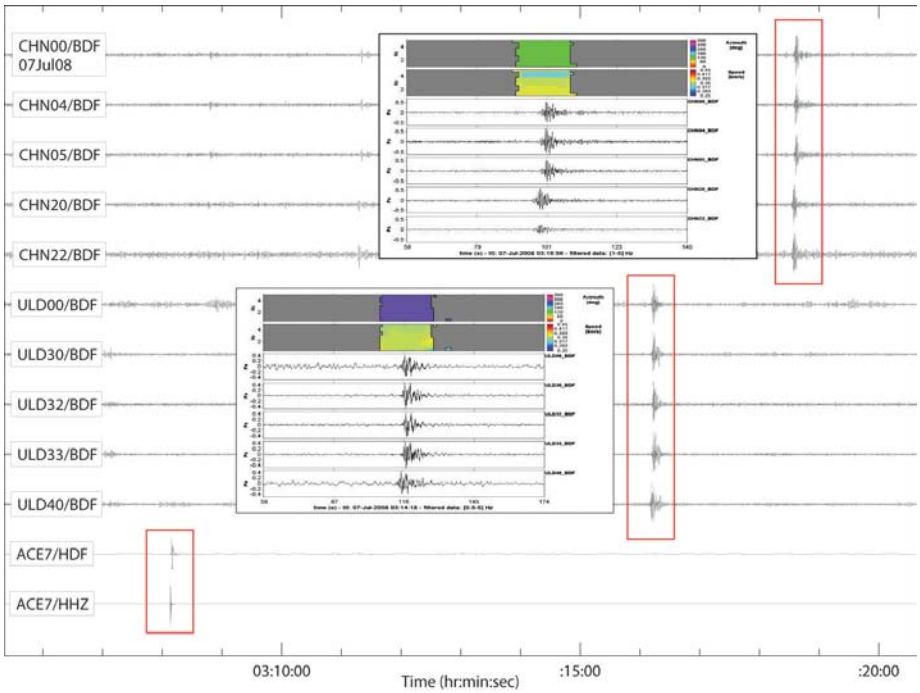

Figure 4. (b) Infrasonic signals and PMCC results for a delay-fired shot at the mine, recorded at CHNAR, ULDAR, and near-field seismo-acoustic station.

Preliminary Analysis of Infrasound Propagation Using the Ground Truth Information

During the two years of sensor operation, the mine conducted 1066 blasts, averaging more than one blast per a day. All blasts were delay-fired shots and the total explosives used were up to 11.2 tons per blast. The temporary stations recorded the near-field seismic and acoustic pressure changes from these blasts, thereby providing data to constrain the exact origin time, location and blast information.

To quantify the seasonal variation in infrasound propagation we used infrasound array observations at two different observation locations, CHNAR and ULDAR. Each array is located at a similar distance from the mine, 181 km and 169 km, respectively. However, the propagation path environments are quite different. CHNAR is located to the NW from the mine, producing a continental path over land. The propagation direction for ULDAR is nearly opposite in direction to CHNAR, eastward from the mine, and across open ocean. Figure 4(b) displays recordings of a delay-fired shot, recorded at the seismo-acoustic arrays (CHNAR and ULDAR), and the temporary station.

Using the complete dataset, we estimated the origin time of each blast from near-field seismic recording, bottom waveform in the figure. We applied the PMCC method to the distant array data to detect the blast-associated infrasonic signals. Wave parameters were estimated and included arrival time, azimuth, apparent velocity, and amplitude of detected signals at each array. Horizontal propagation velocity of infrasound signals, also called celerity, is used not only in infrasonic location, but also infrasonic phase identification. In general, this velocity can be estimated by ray-tracing through a realistic atmospheric velocity model. In the absence of a realistic atmospheric model, the velocity can be estimated using ground truth events with known origin times such as in this study. The horizontal velocities for all the blasts in the ground truth dataset were estimated based on ground-truth source time and infrasound arrival times at both arrays. Figure 5 displays the variation of infrasound travel times from the mine to two arrays over a period of two years.

Based on this analysis we conclude:

- Although propagation distances are similar, travel times of the first arrival (main phase) are significantly different along the paths to the two arrays. For CHNAR, horizontal velocities range from 0.26 to 0.29 km/s corresponding to stratospheric returns. On the other hand, infrasound signals arrive at ULDAR with fast horizontal velocities, ~0.34 km/s corresponding to tropospheric phases.
- For CHNAR, travel times vary systematically with the seasons, arriving up to 68 seconds faster in summertime. Thus, the horizontal velocity showed cyclic variations with velocities near ~0.26 km/s in the winter-spring time, and increasing to ~0.29 km/s in the summertime, and decreasing to ~0.27 km/s in the autumn. This variation in velocity indicates that travel times of infrasound signals can be strongly dependent on seasonal ambient sound velocity structure in the atmosphere.
- The travel times to ULDAR show little seasonal variation. There is some diurnal variation of horizontal velocity. These observations may be a result of the dominant effect of the ocean on temperatures at the ocean-atmosphere boundary.
- These path variations contribute to signal detectability as well. Signals at CHNAR have the highest detectability in the summertime, but many signals were not detected during autumn-winter-spring seasons, even though strong source signals were generated at those times. Compared with CHNAR, detectibility of ULDAR was low only in summer, but stable during the other seasons. Thus the seasonal detectability of the two arrays was opposite to each other, as shown in the figure.

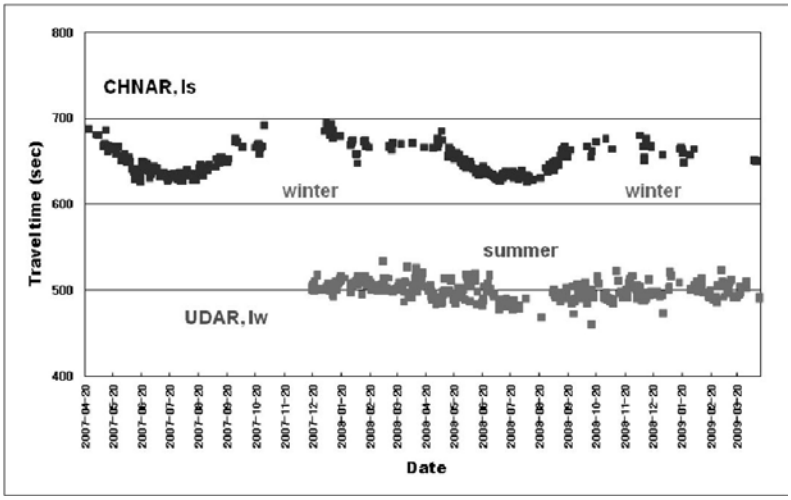

Figure 5. The variation of travel time of infrasound arrivals from the mine to CHNAR and ULDAR during the two years of the ground-truth dataset. Note that ULDAR was installed in December 2007.

CONCLUSIONS AND RECOMMENDATIONS

We have developed the framework for implementing a statistical infrasound event locator. At present, the algorithm is implemented in a Cartesian coordinate system, suitable for local to regional distances, awaiting straightforward conversion to a spherical coordinate system. The algorithm provides a thorough characterization of the source region defined by likelihood contours around the estimated source location. We are in the process of assigning probability values to these contours by numerically integrating the posterior likelihood function (which has a total integral equal to 1). In an example case, we show that the combination of both arrival time and backazimuth constraints results in an improved solution over using either constraint separately.

The preliminary analysis of the ground truth data set indicates that travel times of infrasound strongly depend on seasons as well as path environments. In particular, infrasonic waves to CHNAR propagated as guided waves between the ground and stratosphere. Infrasonic waves to ULDAR also propagated as guided waves, but observed horizontal velocities indicate that wave ducts were formed at relatively lower heights in the troposphere, even though propagation distances to these arrays are similar. The data also show that detectability is dependent on season. Detectability in summer is higher than spring-winter-autumn seasons in the direction to CHNAR with ULDAR showing reverse detectibility. These results indicate that infrasound propagation is related to path environment and seasonal wind in and around the Korean Peninsula. We interpret the time variation in detectability as partially controlled by prevailing periodic winds, northwesterly in the winter and southeasterly in the summer. To investigate these characteristics in detail, further research is required to compare the measured horizontal velocities with predicted ones from atmospheric modeling. These results also illustrate that seasonal and path dependent celerities may improve infrasound location procedures.

ACKNOWLEDGEMENTS

We thank Ryan Modrak for his help in developing and coding the IBL algorithm, and Dale Anderson for patiently explaining Bayesian statistics and for fruitful discussions on how to incorporate infrasound location into a Bayesian framework.

REFERENCES

Arrowsmith, S. J., R. Whitaker, S. Taylor, R. Burlacu, B. Stump, M. Hedlin, G. Randall, C. Hayward, and D. ReVelle (2008a). Regional monitoring of infrasound events using multiple arrays: application to Utah and Washington State, *Geophys. J. Int.* 175: 291–300.

Arrowsmith, S. J., C. Hayward, B. Stump, R. Burlacu, I.-Y. Che, and G. Singh (2008b). Multi-array detection, association and location of infrasound and seismo-acoustic events in Utah in *Proceedings of the 30th Monitoring Research Review: Ground-Based Nuclear Explosion Monitoring Technologies*, LA-UR-08-05261, Vol. 1, pp. 844–852.

Stump, B., R. Burlacu, C. Hayward, K. Pankow, S. Nava, J. Bonner, S. Hock, D. Whiteman, A. Fisher, T. S. Kim, R. Kubacki, M. Leidig, J. Britton, D. Drobeck, P. O'Neill, K. Jensen, K. Whipp, G. Johnson, P. Roberson, R. Read, R. Brogan and S. Masters (2007). Seismic and infrasonic energy generation and propagation at local and regional distances: Phase I – Divine Strake Experiment, *Air Force Research Laboratory*, AFRL-RV-HA-TR-2007-1188.